Analytical Methods

Accepted Manuscript

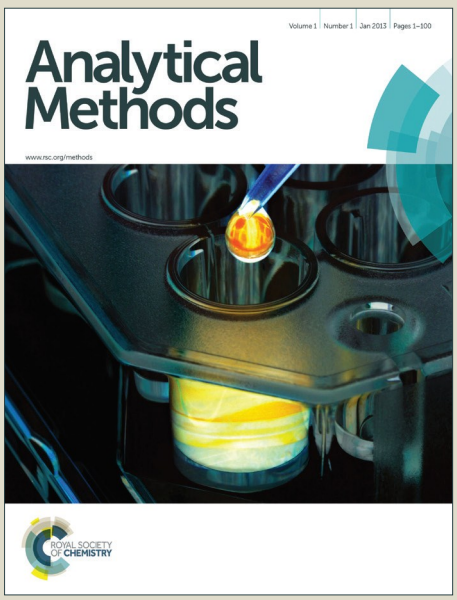

This is an *Accepted Manuscript*, which has been through the Royal Society of Chemistry peer review process and has been accepted for publication.

Accepted Manuscripts are published online shortly after acceptance, before technical editing, formatting and proof reading. Using this free service, authors can make their results available to the community, in citable form, before we publish the edited article. We will replace this *Accepted Manuscript* with the edited and formatted *Advance Article* as soon as it is available.

You can find more information about *Accepted Manuscripts* in the Information for Authors.

Please note that technical editing may introduce minor changes to the text and/or graphics, which may alter content. The journal's standard Terms & Conditions and the Ethical guidelines still apply. In no event shall the Royal Society of Chemistry be held responsible for any errors or omissions in this *Accepted Manuscript* or any consequences arising from the use of any information it contains.

ROYAL SOCIETY OF CHEMISTRY

www.rsc.org/methods

Analytical Methods

ARTICLE

Human Metabolic Responses to Microgravity Simulated in a 45-Day 6° Head-Down Tilt Bed Rest (HDBR) Experiment

Received 00th January 20xx,
Accepted 00th January 20xx

DOI: 10.1039/x0xx00000x

www.rsc.org/

Pu Chen[a], Yanbo Yu[a], Chen Tan[b], Hongju Liu[b], Feng Wu[b], Hongyi Li[b], Jianying Huang[b], Haisheng Dong[b], Yumin Wan, Xiaoping Chen[b]*, Bin Chen[a]*

ABSTRACT: Sustainable human space exploration could progress further with the development of strategies and preparatory activities. However, this progression is largely dependent on ground-based experimental programmes that reflect the limitations of space. The head-down bed rest (HDBR) model simulates the effects of weightlessness on humans. While many physiological indices and their associations with HDBR-induced weightlessness have been well documented in the last several years, the underlying molecular mechanisms remain unknown. Therefore, we used a 6° HDBR model, combined with a metabolomics approach, to reveal novel molecular mechanisms underlying the human responses to weightlessness. A total of 7 volunteers (male, 26.13±4.05 years) were recruited for a standard 45-day HDBR experiment, and their physiological indices associated with bone, muscle, and the gut microbiota were measured. Furthermore, urine samples were collected in nine different phases and analysed using one-dimensional proton nuclear magnetic resonance spectroscopy (^{1}H-NMR) to investigate human metabolic responses to HDBR. The results showed that the urinary excretion of metabolites associated with the deconditioning of bone, muscle and the gut microbiota in response to HDBR changed dramatically over the 45-day experimental period. Meanwhile, the bone, muscle and gut microbiota of the subjects declined after HDBR. Thus, bioinformatics approaches, such as metabolomics analysis, could achieve a more accurate and comprehensive analysis and subsequently provide new insight.

Introduction

Outer space represents an extreme living and working environment to which humans cannot naturally adapt; thus, complex physiological and psychological adaptations are necessary. However, limitations in conducting many physiological experiments in spaceflight have made the interpretation of results difficult. For example, tests are not standardized, there is little control over baseline data, and data are collected from only two or three crew members [1]. These limitations have necessitated an emphasis on the development of ground-based experimental programs. Confinement to bed rest is a valuable analogue for assessing the effects of microgravity, simulated by the induction of physical and physiological changes similar to those observed after humans are exposed to actual spaceflight. The 6° HDBR model is one of the most effective analogues for spaceflight microgravity [2]. Despite the extreme variability in experimental conditions and mission activities associated with spaceflight, the quantitative and qualitative comparisons with this bed rest analogue are striking.

In addition, HDBR is an appropriate experimental model for inducing the effects of microgravity on the human body. In comprehensive comparisons, body weight, muscle strength, muscle mass, plasma volume, bone density, gut calcium absorption, urinary calcium, renal stone risk, and insulin resistance show a similar degree of change under bed rest and spaceflight [3]. Moreover, HDBR may induce pain and psychosomatic reactions experienced in microgravity [4].

Bone resorption, amyotrophia, and cardiovascular problems are three prominent issues observed in spaceflight and HDBR. For example, actual and simulated microgravity can induce changes in cardiac structure and function that affect the entire cardiovascular system, resulting in orthostatic intolerance and a reduced aerobic capacity [5, 6]. Sixty days of 6° HDBR were shown to induce a reduction of cardiac systolic and pumping functions and decrease cardiopulmonary functional reserves and exercise capacity [7]. To protect astronauts from the undesirable effects of microgravity, many strategies have been tested and well documented; among these strategies, exercise is widely used to cope with the declining muscle strength observed under adaptation to microgravity [8]. However, the underlying molecular mechanisms associated with these biological processes have not been well documented until recently. These mechanisms greatly impact the outcomes of

[a] Key Laboratory of Space Nutrition and Food Engineering, China Astronaut Research and Training Centre, No. 26, Beijing Road, Beijing 100094, China.
[b] State Key Lab of Space Medicine Fundamentals and Application, China Astronaut Research and Training Center, No. 26, Beiqing road, Beijing 100094, China.
[c] †*Corresponding authors
Bin Chen, E-mail address: chenb12@aliyun.com; Xiaoping Chen, E-mail address: xpchen2009@163.com.
Electronic Supplementary Information (ESI) available: [Two tables and figures are presented in supplementary information]. See DOI: 10.1039/x0xx00000x

countermeasures against microgravity and limit the accurate evaluation of the effects of pathophysiological stimuli associated with weightlessness.

However, metabolic phenotyping and metabolome-wide association studies offer a powerful new method for discovering the molecular biomarkers and metabolic pathways underlying physiological changes [9]. In particular, nontargeted profiling and comprehensive analyses of the metabolites in biofluids provide a final readout of genetic modifications or protein expression [10]. Combination of this technology with appropriate multivariate statistical analysis can provide metabolic profiles and molecular insights to facilitate the understanding of relevant metabolic variations of physiological perturbations [11]. Furthermore, compared with other omics approaches, metabolomics provides a broad scope of direct information on integrated cellular responses, with low demand regarding material and sample preparation [12]. Hence, metabolomics offers the best trade-off and has become a popular method for metabolic discovery. In addition, metabolite levels are sensitive to changes in both metabolic fluxes and enzyme activity [13]. Thus, these molecules can serve as diagnostic indicators to monitor all events affecting metabolism.

NMR spectroscopy and mass spectrometry are the two major techniques used for metabolic analysis. NMR is a powerful approach for both the identification and quantification of analytes with a number of important advantages, including high reproducibility, high-throughput, non-destructive, non-biased analyses, no requirement for chromatographic separation, and, most importantly, minimal requirements for sample preparation [14, 15]. In addition, unlike gas or liquid chromatography-mass spectrometry (GC/LC-MS) methods, no chemical derivatization or ionization is necessary. NMR is particularly suitable for the detection of polar and uncharged compounds, such as sugars, amines or relatively small volatile compounds (such as formic acid, formaldehyde, and acetone), which are frequently undetectable using LC-MS methods. Moreover, multidimensional and heteronuclear NMR techniques can be employed for the unambiguous identification and characterization of unknown compounds [16, 17]. However, the inherent low sensitivity of NMR restricts the detection limit to approximately 1 μM and often necessitates the use of a relatively large sample volume (~200-500 μL). In the present study, we conducted metabolic profiling using a 6° HDBR model to reveal the molecular mechanisms underlying the response to weightlessness. To our knowledge, this study is the first to conduct metabolic profiling using HDBR experiments, and the results showed that physiological parameters associated with bone resorption, muscle turnover, and gut microbial activities were altered, but these changes were not significant. In contrast, the urinary excretion of metabolites associated with the observed physiological deconditioning was remarkably altered, suggesting declines in bone, muscle, and the gut microbiota under HDBR during the 45-day experimental period.

Materials and Methods

HDBR Experiment

A total of 7 male volunteers were randomly recruited in China and sent to a screening commission for a special physical examination and psychological assessment prior to the HDBR experiment. All of the subjects were healthy nonsmokers who did not exhibit regular drug intake or antibiotic use. The mean age, body weight, and height of the subjects were 26.13±4.05 years, 64.0±6.14 kg, and 171.8±3.0 cm, respectively. All of the participants were subjected to standardized -6° HDBR; i.e., the subjects were positioned with a continuous head-down tilt in a strict -6° supine position under 24 h supervision for 45 days. Two or three individuals were housed together in a room with beds separated by movable curtains. All of subjects ate, slept, and washed in a strict HDBR environment, and their dietary items, daily schedule, and life styles were well controlled during the 45-day bed rest period.

The study was conducted at the China Astronaut Research and Training Centre in four phases: (1) a 7-day preliminary test, (2) a 6-day pre-HDBR procedure, (3) 45 days of HDBR, and (4) a 10-day post-HDBR process. A preliminary test was conducted to ensure that all experimental contents and procedures were familiar to the subjects. Urine specimens were collected in 9 time courses for metabolomics analyses: 2 days prior to HDBR (R-2); 2 days after HDBR (R02); and 4, 14, 21, 37, and 44 days after HDBR, indicated as R04, R14, R21, R37, and R44, respectively. Additionally, another batch of urine samples was collected on the 7th day of the 10-day post-HDBR process (R+7). All samples were aliquoted into sterile microcentrifuge tubes and stored at -80°C. During the experimental period, all of the subjects were confined to a typical hospital environment. All participants provided written informed consent. The protocol was conducted in accordance with the principles of the Declaration of Helsinki and approved by the medical ethics committee of the China Astronaut Research and Training Centre.

Physiological Assessments

Bone mineral density (BMD)

Changes in bone mineral density were assessed using dual energy X-ray absorptiometry (DEXA) at R-2, R15, R30, R44, and R+10 [18]. In addition, serum biochemical markers of bone turnover, including bone alkaline phosphatase (BALP), procollagen type I C-terminal propeptides (PICP), osteocalcin (OC), and tartrate-resistant acid phosphatase (StrACP), were also measured using enzyme-linked immunosorbent assays (ELISAs) at R-2, R07, R14, R30, and R44. Muscle volume was measured using magnetic resonance imaging (MRI) at R-5 and R+1 [19].

Aerobic Bacterial Counts

Faeces samples were collected from volunteers to determine the aerobic bacterial counts of *Lactobacillus* spp. and *Bifidobacterium* spp. at R-2, R02, R04, R07, R14, R21, R30, R35, R45, R+3, and R+7. A total of 1 g of faeces was diluted with 9 mL of sterile normal saline to 0.85%, and the mixture was vibrated for 2 min. The mixture was further diluted to multiple concentrations ranging from 10^{-1}~10^{-7}, and 1 mL of the diluted

mixture was added to plate count agar medium, which was then mixed well. Subsequently, the strain cultures were inverted and incubated for 48 h at 37°C under anaerobic conditions [20].

^{1}H-NMR Experiment

A 40 µL urine sample was diluted with 20 μL of 0.2 M sodium phosphate buffer (pH 7.4±0.5, 0.01% sodium 3-(trimethylsilyl) propionate-2,2,3,3-d4 (TSP), 3 mM Na_3N, 25% D2O), followed by centrifugation at 12,000 *g* for 10 min at 4°C. After centrifugation, 50 µL of the supernatant was transferred to a microtube (1.7-mm outer diameter), pending NMR analysis. ^{1}H NMR spectra were obtained for all samples using a Bruker DRX 600 MHz spectrometer (Bruker Biospin, Rheinstetten, Germany) with a 5-mm TXI probe at 600.13 MHz. The temperature was maintained at 298 K. The urine spectra were processed using phosphate buffer to lock the field. A standard one-dimensional (1-D) NMR pulse [(NOSEYPR1D, recycle delay (RD)-90°-t_1-90°-t_m-90°-acquire free induction decay (FID)] was employed for the acquisition of all spectra. The water peak was suppressed by selective irradiation during an RD of 2 s, a mixing time (t_m) of 100 ms and a fixed t_1 of 3 μs. The 90° pulse length was adjusted to approximately 10 μs. A total of 256 scans were recorded to obtain 64 k data points with a spectral width of 20 ppm. An exponential function was applied to the FID prior to Fourier transformation to achieve line broadening of 0.3 Hz [21].

Data Preprocessing

The transformed NMR spectra were automatically corrected for phase and baseline distortions and calibrated (TSP singlet at 0.00 ppm) using MestraReNova 10.0.2 (Bruker Biospin srl). The spectral data (from δ 0.5 to δ 9.5) were digitalized onto 1480 data points with a spectral width of 0.005 ppm. Spectral regions containing water (δ 4.62-5.17) and urea (δ 5.57-6.15) peaks or only noise (δ 0–0.5) were removed from each spectrum to eliminate the variability associated with the unwanted noise. Metabolite assignments were obtained after matching the recorded signals with published NMR spectral [10, 22] and the Human Metabolome Database (HMDB) using Chenomx NMR Suite 8.1.

Multivariate Analysis

The NMR spectral dataset derived from the 45-day HDBR experiment were further analysed using SIMCA-P+ (version 14, Umetrics) statistical NMR data analysis software. Subsequently, a principal components analysis (PCA) model was employed to identify and explain 'clustering', trends and 'outliers' based on the normalized dataset. All outliers were excluded, and an orthogonal partial least squares discriminant analysis (O2PLS-DA) model was built to exclude the noise from inter-individual variations. The goodness of fit of the O2PLS-DA model was further validated using a permutation test with 200 iterations and 7-fold cross-validation. Subsequently, the VIP value derived from the O2PLS-DA model was used to screen candidate biomarkers showing significant changes according to the examined periods. Metabolites exhibiting VIP > 1 in the O2PLS-DA model were further analysed using one-way ANOVA, with significance based on an *alpha* level of 0.05 [23]. Furthermore, the spectral data from three representative sampling times (R02, R21, and R44) selected based on the O2PLS-DA model were compared with R-2 using the S-line plot of O2PLS-DA, and Pearson correlation coefficient values were compiled to discriminate metabolites between the urine samples collected on three days (R02, R21, and R44) and at R-2. To facilitate reading, a cut-off value of 0.6 was used to retain the most relevant features.

Results and Discussion

Metabolic Profiles Associated with HDBR

***^{1}H-NMR Peak Assignment*.** To investigate the specific metabolic signature associated with HDBR-induced psycho-physiological changes, we acquired urinary metabolic profiles over a period of 45 days. Four representative ^{1}H NMR urinary spectra obtained from the samples collected at R-2, R02, R21, and R44 are presented in **Figure 1a** and **b**. As shown in **Figure 1**, a total of 23 metabolites were assigned, indicating the strong impact of HDBR on the urine composition.

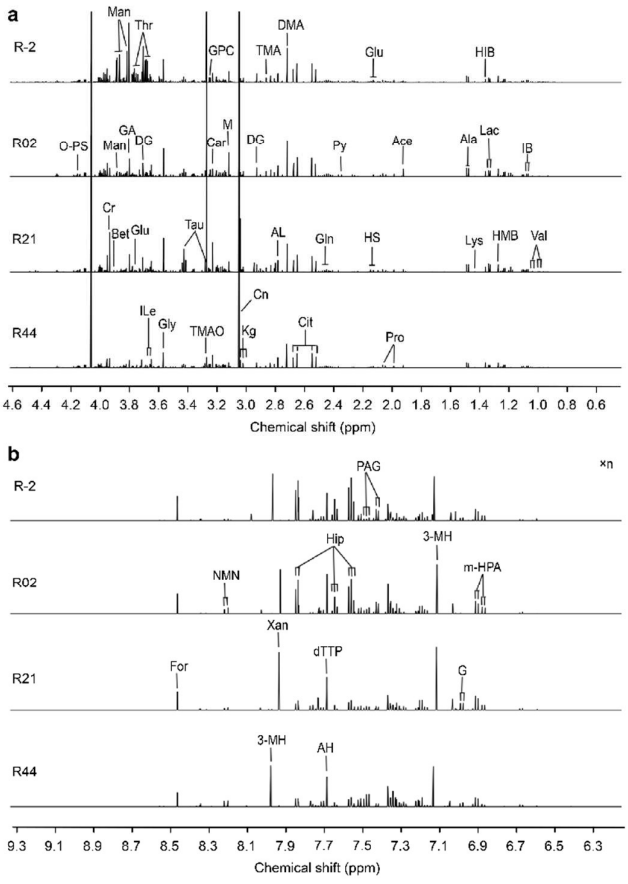

Figure 1. Urinary 600 MHz 1H NMR spectral data (δ 0.5-4.6 and δ 6.2-9.3) obtained during different time courses. The following key abbreviations are used: Tau, taurine; Cn, creatinine; TMAO, trimethylamine N-oxide; GA, guanidoacetate; Man, mannitol; Gln, glutamine; Ans, anserine; Glu, glutamate; Cys, cysteine; Car, carnitine; DG, N,N-dimethylglycine; GPC, glycerophosphoryl-

choline; Py, pyruvate; Cr, creatine; Gly, glycine; Cit, citrate; 5-HT, serotonin; Hip, hippurate; Ace, acetate; Ala, alanine; AH, aminohippurate; Xan, xanthine; For, formate.

Metabolic Responses to HDBR over 45 Days. We first examined the changes in metabotypes in metabolic space during HDBR. For this purpose, two pattern recognition techniques that are widely used in metabolic analyses were selected-principal component analysis (PCA) and orthogonal partial least squares-discriminant analysis (O2PLS-DA). PCA and O2PLS-DA are two of the most widely used techniques in metabolic research, for they are outstanding in exploring class differences and highlighting explanatory variables. Moreover, these methods allow us to project the high dimension data into a low dimensional space for easier interpretation and visualization. This space is described by latent variables which consists of a linear combination of the original variables. Furthermore, these variables are irrelevant, for they are orthogonal to each other. In PCA model, which generates new variables (generally referred to as principal components, PCs) via linear combinations of the starting variables with appropriate weighting coefficients. Thus, the model describes the space corresponding to the highest variance of the data, which is useful for the observation of clustering trends, identification of outliers, and screening of variables [24]. Whereas in O2PLS-DA the space corresponds to that with the highest covariance between the data and the response variable indicates class membership, thus producing a model in which class separation is emphasised. What's more, loadings from these models can give easy access to information about which variables are influencing the variation seen between the samples. As demonstrated by the scatter plot of the PCA scores in **Figure S1**, no obvious clustering information was obtained for the overlapping sample points. Thus, the PCA approach could not be used for biomarker screening because too many inter-group variances were derived, which obscured the extra-group variances. Therefore, the O2PLS-DA model was used to investigate metabolic changes.

O2PLS-DA is a supervised pattern recognition model based on an extension of the PLS algorithm, which requires splitting the variation of the predictor variables into two parts: variation orthogonal (uncorrelated) to the response and variation correlated with the response. While the predictive accuracy remains the same as that of conventional PLS, after separating the variation using O2PLS-DA, the interpretation of the model can be improved [24]. The data matrix could therefore be visualized in a simple graphic (**Figure 2a**) to show that all of the sampling points were clustered into four groups: the samples from 2 days before HDBR (R-2); 2 and 4 days after HDBR (R02 and R04); 21 days after HDBR (R21); 14, 30, 37, and 44 days after HDBR (R14, R30, R37, and R44); and 7 days post-HDBR (R+7). When viewed holistically, these four groups could be further divided based on the first PC. Additionally, compared with the samples from R-2, the samples from R21 were closest in the metabolic space constructed using the first two PCs, followed by the samples from R02 and R04 and the samples from the last group, which were farthest. However, the slightly lower accuracy obtained using the O2PLS-DA model with a Q^2 value of 0.115 reflected the fact that individual differences affect human experiments, although the dietary items and environmental conditions were well controlled in the present study. Hence, the interpretative ability of the O2PLS-DA model was validated

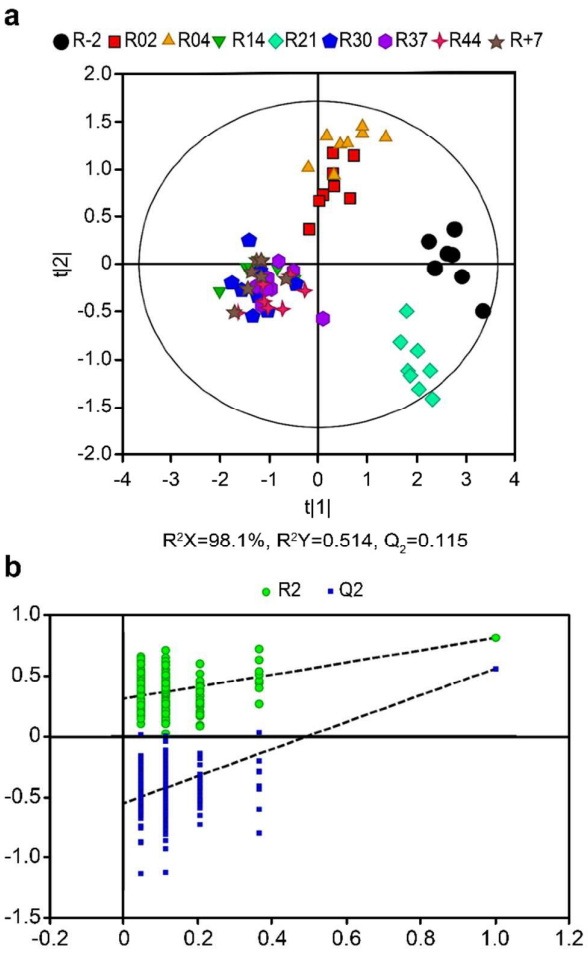

Figure 2. O2PLS-DA score plot of the urinary 1H NMR spectral data obtained during 45 days of -6° head-down bed rest (HDBR) (a). R-2 refers to 2 days before HDBR, while R02, R04, R14, R21, R30, R37, and R44 represent urine specimens collected on the 2nd, 4th,…, and 44th days of bed rest, respectively, and R+7 refers to the samples collected on the seventh day after HDBR. Scatter plot of the results obtained from a permutation test with 200 iterations (b). R2, variation orthogonal (uncorrelated) to the response, and Q2, variation correlated with the response. The vertical axis shows the R2Y and Q2Y values of each model, and the horizontal axis represents the correlation coefficient between the permuted Y-vectors and the original Y-vector. This plot displays the correlation coefficient between the original Y and the permuted Y versus cumulative R2 and Q2.

using a permutation test with 200 iterations. As shown in **Figure 2b**, all of the Q^2 values indicated in blue on the left were lower than the original points indicated on the right, and the blue regression line of Q^2 points intersects the vertical axis (on

the left) below zero, indicating that the original model was valid.

These differences manifested in the O2PLS-DA scores plot as driving the variation in the first PC. Therefore, the most discriminating metabolites were screened based on the VIPs of the first PC from the O2PLS-DA model with a criterion of VIP > 1. The above screened metabolites were further examined

using one-way ANOVA and post-hoc analysis, and the results are summarized in **Table 1**.

Three representative sampling times (R02, R21, and R44) were selected from the four groups divided based on the O2PLS-DA model, and these three urine samples were subsequently compared with the samples obtained for R-2 using the OPLS-DA model **(Figure S2)**. Moreover, the most correlated discriminatory metabolites were selected based on the Pearson correlation coefficient, with a cut-off value of 0.6, and the results are shown in **Figure 3** and **Table S1**. These metabolites, accounting for the sequential changes in physiological variables corresponding to a series of disparate HDBR time courses, suggest a new underlying molecular mechanism associated with HDBR.

Urinary Excretion Patterns of Metabolites Associated with Bone Adsorption

We next investigated whether the metabolites identified above reflected an underlying physiological mechanism.

We found that the level of *L*-threonic acid excretion rapidly decreased at R02, with a p value of 3.51×10^{-10} (**Table S2**), followed by a slight increase at R04 and a decrease at R14 and

Table 1. Summary of Metabolites with VIP > 1 in the O2PLS-DA Models for Different Days

	Chemical shift	VIP	ANOVA[a]	
Metabolites	δ/ppm	OPLS-DA	p value	FDR
Trimethylamine N-oxide	3.28(s)	18.185	1.90E-07	7.12E-07
Creatinine	3.05(s)	13.751	2.72E-03	6.81E-03
Guanidoacetate	3.80(s)	3.840	3.98E-11	2.98E-10
Mannitol	3.85(m)	-	-	-
Threonate	3.70(m)	3.388	1.61E-11	2.42E-10
Taurine	3.43(t)	1.196	1.09E-02	2.04E-02
Glycerophosphoryl choline	3.27(s)	2.005	1.82E-04	5.46E-04
Pyruvate	2.35(s)	1.347	-	-
Creatine	3.94(s)	1.461	-	-
Glycine	3.57(s)	1.325	-	-
Citrate	2.66(dd)	1.293	-	-
m-HPA	7.12(d)	1.106	-	-
Hippurate	7.56(t)	1.039	-	-
Betaine	3.26(s)	1.279	3.75E-03	8.03E-03
Glutamine	2.28(m)	1.200	1.90E-07	7.12E-07
Dimethylamine	2.72(s)	1.174	-	-

[a]One-way analysis of variance (ANOVA) was used to determine the p value, with Fisher's least significant difference method (Fisher's LSD) and Tukey's honestly significant difference (Tukey's HSD). $p > 0.05$ indicates no significant difference; 14 metabolites showed p values < 0.05;

Abbreviations: s, singlet; d, doublet; t, triplet; m, multiplet; dd, doublet of doublets; "-", not available; *m*-HPA, *m*-hydroxyphenylacetate

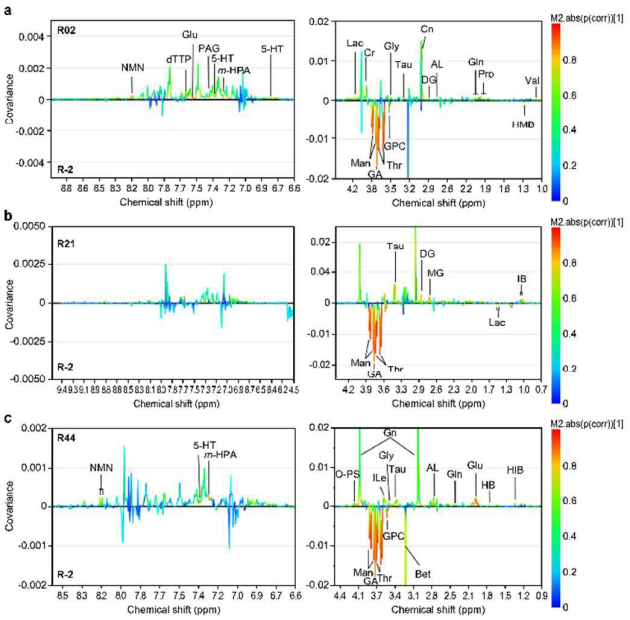

Figure 3. S-line plot derived from the OPLS-DA model based on the 1H NMR spectra of two phases during 45 days of -6° head-down bed rest (HDBR). In each plot, the y coordinate and the colour scale depict the covariance and correlation between each variable and the class, respectively. Specifically, as the colour of the peak gradually changes from blue to red, the absolute value of Pearson's correlation coefficient increases from 0 to 1, indicating the resonances important for discriminating the urinary profiles of pairwise sampling times during HDBR. The three sub-Figures show a comparison of the results obtained at R02 (a), R21 (b), and R44 (c) with R-2.

R21, with a p value of less than 0.05. However, the level of *L*-threonic acid excretion increased at R30 and R37 and decreased at R44 and R+7, with a p value higher than 0.05 (**Figure 4a**). *L*-Threonic acid is an active vitamin C metabolite. Vitamin C is a marker of osteoblast formation, which stimulates procollagen and enhances collagen synthesis [25]. Therefore, *L*-threonic acid might play a role in mineralization via its positive action on vitamin C. The significant decrease in *L*-threonic acid excretion observed during the 45 days of HDBR might reflect two potential mechanisms: increasing *L*-threonic acid utilization for collagen synthesis and decreasing *L*-threonic acid adsorption. In addition, increasing *L*-threonic acid excretion might reflect the stress induced by HDBR. However, compared with R-2 (the day before HDBR), the remain 8

sampling times showed a remarkable reduction, with a significant *p* value of less than 10^{-6}, suggesting a dysfunction in bone mineralization. Bone adsorption in a weightless environment has previously been reported during both actual spaceflights [26] and HDBR experiments [27]. However, the underlying molecular mechanisms have not been well documented. The results of the present study indicated that a barrier in the *L*-threonic acid metabolic pathway might be responsible for the observed bone adsorption.

Urinary Excretion Patterns of Metabolites Associated with Muscle Mass

Glutamine is the most abundant free amino acid in muscle, and at the last 8 time points except for R21, lower levels of glutamine excretion were observed, with a *p* value of less than 0.004753 (**Figure 4b** and **Table S1**). Typically, a balance between the excretion and adsorption of glutamine is maintained in muscle, and glutamine is one of the most important amino acids derived from intermediate metabolism during catabolism, particularly in muscle cells [28]. Thus, a reduction in the excretion of glutamine might reflect a decrease in the total muscle mass. Furthermore, creatinine levels differ with meat consumption, and the urinary creatinine excretion rate is an established marker of muscle mass [29]. Furthermore, 24-hour urinary creatinine excretion is typically examined to estimate the total-body skeletal muscle mass. Hence, creatinine could be selected as a robust indicator of muscle turnover [30]. Thus, as expected, creatinine exhibited a sustained increase across the examined time course **(Figure 4c),** but this increase was not significant, with a *p* value larger than 0.05 **(Table S1)**. Glycine, which is required for the biosynthetic precursor of creatine [31], was slightly increased at R14, R21, and R30 compared with R02 or R04 (**Figure 4c**). This increased glycine excretion might therefore reflect a higher requirement for creatine synthesis during this time course. Guanidoacetate is an intermediate metabolite, from which creatine is formed via methylation, accounting for the observed muscle creatine accumulation [32]. As shown in **Figure 4c**, the urinary excretion of guanidoacetate was significantly decreased compared with the day before HDBR (R-2), and this effect might reflect a decrease free amino acid production in muscle (e.g., glutamine). Taken together, changes in the urinary excretion of glutamine, creatinine, glycine, and guanidoacetate might reflect an enhancement of protein turnover, further inducing muscle turnover.

Urinary Excretion Patterns of Metabolites Associated with Cardiovascular Function

The VIPs obtained from the O2PLS-DA model for the 45-day HDBR dataset (**Figure 2a**) showed that the first PC predominantly consisted of trimethylamine-*N*-oxide (TMAO, VIP = 18.185), representing the greatest source of variation. As shown in **Figure 4d**, urinary TMAO significantly decreased at 2 days after HDBR ($p = 2.42 \times 10^{-4}$), then increased at R04 and decreased at R14 ($p = 0.036$). Furthermore, urinary TMAO increased markedly at R21 ($p = 9.77 \times 10^{-6}$) and subsequently varied in a pattern similar to that observed for the first four sampling times (from R-2 to R14), compared with the samples obtained from R21 to R44. In addition, a similar level of urinary TMAO excretion was observed at 7 days post-HDBR compared with R44. TMAO is a hepatic oxidation product of dietary amines (specifically TMA), and this molecule causes many cardiovascular diseases, such as heart attack, stroke, and atherosclerosis [33]. Thus, TMAO is pro-atherogenic. TMA is metabolized from choline by gut microbes [4]. Notably, choline can be metabolized from glycerophosphorylcholine (GPC) in the gut; GPC was slightly increased at R02, significantly reduced at R04 ($p = 0.017$), and sustained at R14. In addition, GPC showed a remarkable increase at R21, returned to a level comparable to the R14 level at R30, and was subsequently sustained at the remaining three sampling times (R37, R44, and R+7) (**Figure 4e**). Furthermore, GPC can also be metabolized to betaine, and betaine further promotes the methylation of homocysteine in plasma, which is a risk factor for cardiovascular problems [34]. Additionally, betaine can be metabolized to glycine. As shown in **Figure 4e**, betaine exhibited variations similar to its metabolic precursor (GPC). Specifically, betaine increased from R-2 to R02, then gradually decreased from R02 to R14, increased greatly from R14 to R21, and finally decreased from R21 to R+7. Moreover, taurine showed a continuous increase from R-2 to R21 and a decrease from R21 to R+7 (**Figure 4e**). Taurine is a free amino acid in the human body and has positive effects on the human cardiovascular system, reflecting the reduction of lipid and reactive oxygen species (ROS) mediated by this free amino acid. Furthermore, taurine promotes the down-regulation of angiotensin II and angiotensin-converting enzyme (ACE) and the up-regulation of *NO*, further accelerating the contraction of the heart [35]. Thus, taurine exerts many protective effects on the cardiovascular system. In addition, elevated urinary taurine excretion might reflect the reduced utilization of this molecule and could result in cardiovascular system dysfunction, as lipid and reactive oxygen species may be increased, and *NO* might be down-regulated. In addition, the level of urinary mannitol during the 45-day HDBR experiment showed a strong ($r \geqslant 0.9$) negative correlation with R-2 (**Figures 3a-c**). Mannitol absorbs water molecules from plasma, functioning as a vasodilator, typically dilating blood vessels and preventing platelets from becoming sticky [36]. Thus, decreased urinary mannitol excretion might result from the increasing use of this molecule as a regulatory factor. Interestingly, a previous 45-day HDBR experiment was conducted to examine cardiovascular effects, and the results showed changes in a series of cardiac parameters during HDBR on days -2, 11, 20, 32, 40, and +8, including heart rate (HR), pulse rate (PR), high heart rate variability (H_HRV), low heart rate variability (L_HRV), balanced heart rate variability (B_HRV, the ratio of low heart rate variability to high heart rate variability), systolic blood pressure (SBP), and diastolic blood pressure (DBP). In this experiment, HR was decreased at day 11 compared with 2 days pre-HDBR, then gradually increased from day 11 to 8 days post-HDBR. However, the other parameters showed different alterations [37]. HOwever, these variables, which indicate cardiovascular issues, were not considerably altered and were maintained within normal

physiological ranges. In the present study, we observed that the urinary excretion of associated metabolites, such as TMAO, GPC, betaine, taurine, and mannitol, changed markedly during the 45-day HDBR experiment, suggesting the onset of cardiovascular problems. Thus, these metabolites might be selected as candidate biomarkers for prognostic cardiovascular deconditioning.

Changes in Mammalian-Microbial Cometabolites

Urinary *m*-hydroxyphenylacetate (*m*-HPA) and hippurate are predominantly gut microbial products of animal dietary protein metabolism. As shown in **Figure 4f**, *m*-HPA was increased at R02 compared with R-2, then slightly decreased from R02 to R14,

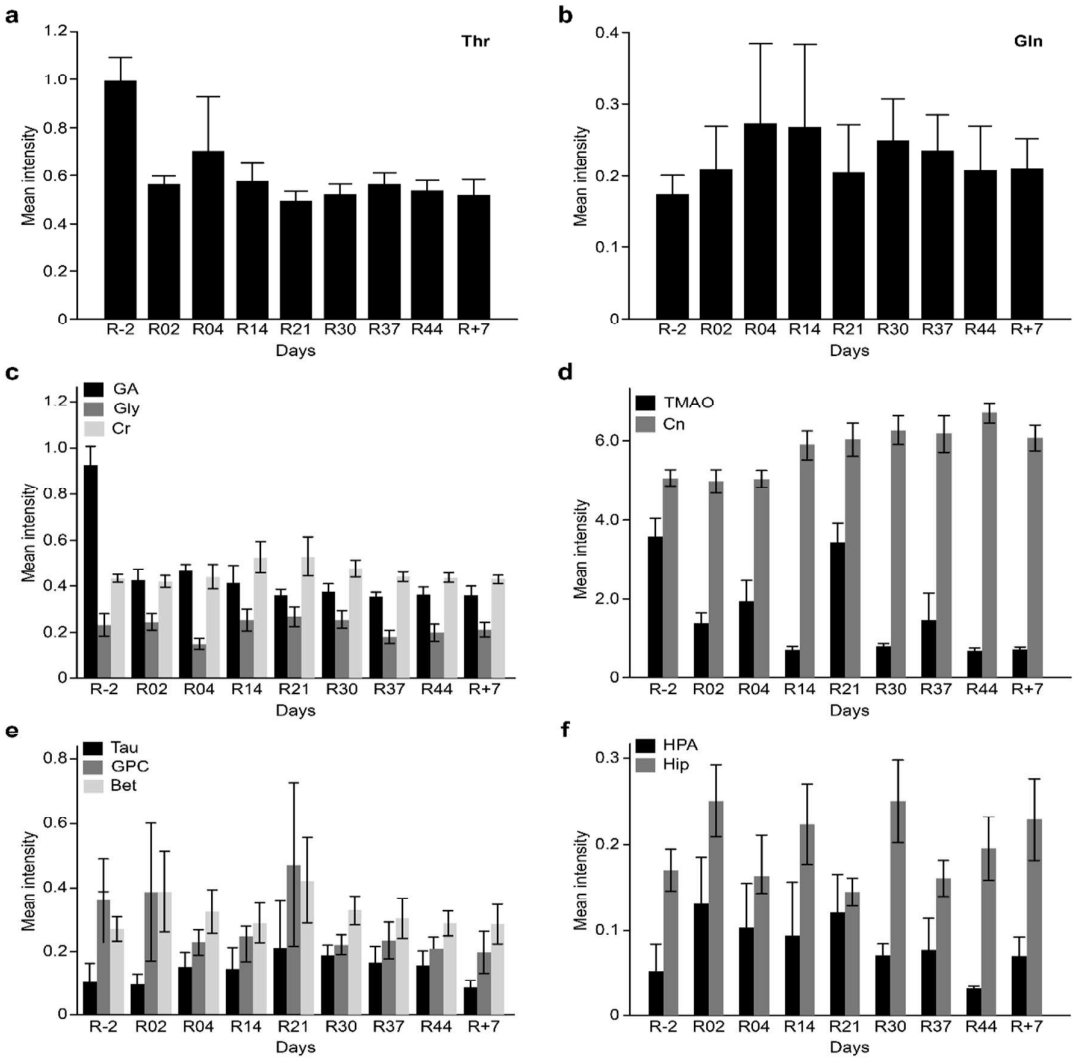

Figure 4. Urinary excretion pattern of the metabolites screened using the O2PLS-DA model.

increased at R21, decreased at R30, increased at R37, decreased at R44, and increased at R+7. Thus, the urinary excretion levels of *m*-HPA were high overall during the 45-day HDBR experiment. However, these changes were not remarkable.

The fermentation of amino acids mediated by *Clostridium spp.* and *Bacteroides spp.* typically produces a series of phenolic and indolic compounds, among which *m*-hydroxyphenylacetate (*m*-HPA) is a by-product of tyrosine metabolism mediated by *Clostridium spp.* [38]. Furthermore, *m*-HPA can be metabolized to *p*-cresol by *Lactobacillus* spp. [39]. p-Cresol has an impact on renal failure, in addition to its impact on endothelial function, and serves as a marker of cardiovascular disease, which is a leading cause of mortality in patients with chronic renal failure [40, 41].

Effects of HDBR on Bone, Muscle, and the Intestinal Flora

The metabotypes of the volunteers significantly changed during HDBR, suggesting multiple physiological responses of human variables. To characterize the precise changes in human variables and compare the metabolic profiles with physiological

Analytical Methods

ARTICLE

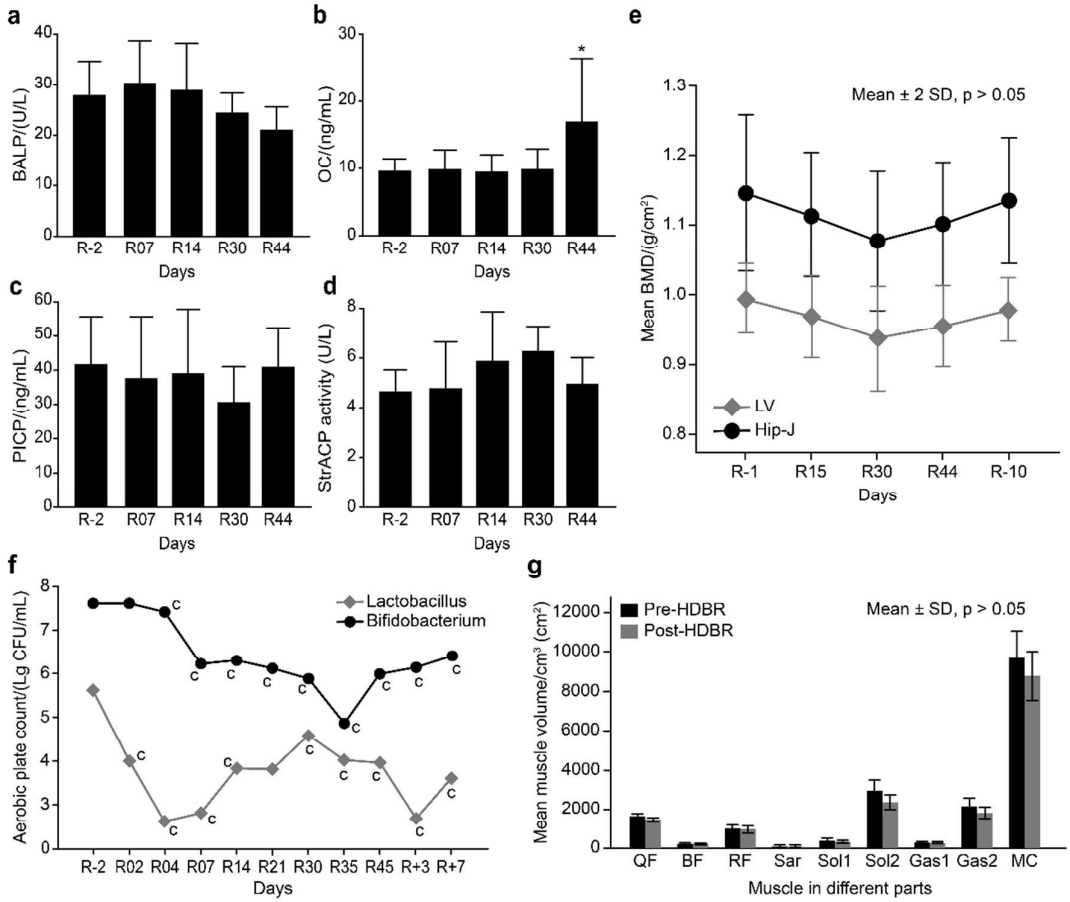

Figure 5. Bar plot of the physiological indices associated with bone resorption (a-e), gut-microbial activity (f), and muscle turnover (g). The following markers are associated with bone resorption: BALP, bone alkaline phosphatase, PICP, procollagen type I C-terminal propeptides, OC, osteocalcin, StrACP, tartrate-resistant acid phosphatase, BMD, bone mineral density, LV, lumbar vertebra or lumbar spine; Hip-J, hip joint. The following markers are associated with muscle turnover: volume of the QF (quadriceps femoris muscle), BF (biceps femoris muscle), Sar (sartorius muscle), Sol1 (soleus muscle), and Gas1 (gastrocnemius muscle); and maximum cross-sectional area of the RF (rectus femoris muscle), Sol2 (soleus muscle), Gas2 (gastrocnemius muscle), and MC (middle crus).

data, we examined multiple human physiological parameters, including bone resorption, gut-microbial activity, and muscle turnover. The results are summarized in **Figure 5**.

Effects of HDBR on Bone. To examine changes in bone activity and function, four serum biomarkers of bone formation (bone alkaline phosphatase (BALP), procollagen type I C-terminal propeptides (PICP), osteocalcin (OC), and tartrate-resistant acid phosphatase (StrACP)) were measured. In addition, bone mineral density (BMD) was evaluated. As shown in **Figure 5a,** the activity of BALP was slightly increased at R07 and R14 and then gradually decreased. The concentration of OC at R07, R14, and R30 was sustained at a level similar to that at R-2. However, the OC concentration significantly increased at R44 (**Figure 5b**). Moreover, the serum PICP concentration slightly decreased at R07 and R30 and subsequently recovered to a level similar to the R-2 level at R44 (**Figure 5c**). In addition, StrACP activity increased from R-2 to R30 and recovered at R44 (**Figure 5d**), and bone mineral density decreased from R-2 to R30, and then increased from R30 to R+10 (**Figure 5e**). R+10

showed a recovery period of 10-days post-HDBR, and BMD recovered to a level similar to that at R-2. Previous studies have demonstrated that coupled bone formation and bone resorption is a dynamic process that occurs throughout life. While BMD reflects the combination of the peak bone mass and the amount of subsequent bone loss, changes in bone turnover markers occur more rapidly and provide a dynamic view of current bone metabolism [42]. BALP is a marker of increased osteoblast activity, and this molecule is secreted from bone-forming osteoblasts [43]. Osteocalcin, the second most abundant protein in bone after collagen, is secreted from osteoblasts and has been implicated in mineralization and calcium ion homeostasis [42]. PICP levels have been used to estimate the rate of type I collagen synthesis in the body, and the serum concentration of PICP is correlated with the rate of bone formation [44]. Therefore, the serum concentration of PICP can be used as a biomarker of bone remodelling. Bone resorption results in the release of StrACP from osteoclasts, and bone StrACP might act as a suitable biochemical probe for osteoclast function [45]. Thus, these biochemical markers of bone metabolism can be divided into biomarkers of formation and resorption. Formation markers include enzymes secreted from osteoblasts during bone formation, such as BALP, OC, and PICP . Bone resorption markers are generated from the breakdown of type I collagen during bone resorption and include specific enzymes secreted with *Lactobacillus*. The gut microbiota are associated with various essential biological functions in humans via a microbial-host co-metabolism "network" to cope with stresses and modulate the activities of multiple pathways in organ systems associated with different physiological problems caused by HDBR.

Effects of HDBR on Muscle. Extensive evidence has shown that hypomotility is a major challenge for humans under both simulated microgravity and actual space flight [1]. In a weightless environment, humans require little energy to cope with minimum forces from the Earth, resulting in a reduction of the musculature system. In the present study, the volumes or areas of muscles from different parts of the body were measured and described with an error bar plot (**Figure 5g**). As expected, the total volume of the quadriceps femoris muscle (QF), biceps femoris muscle (BF), sartorius muscle (Sar), soleus muscle (Sol1), and gastrocnemius muscle (Gas1) was decreased after 45 days of HDBR. The maximum cross-sectional area of the rectus femoris muscle (RF), soleus muscle (Sol2), gastrocnemius muscle (Gas2), and middle crus (MC) was also reduced after HDBR. Nevertheless, these effects were not significant in the context of normal homeostasis in the human body.

Association between Metabolic Profiles and Physiological Parameters

Previous studies on ground-based weightlessness have only focused on a few physiological parameters, reflecting limitations in analytical approaches, and the results have been far from satisfactory, reflecting normal homeostasis in the human body. This barrier has inhibited progress in the development of protective strategies for safe space travel. With the advent of analytical approaches and data preprocessing for bioinformatics, the systematic identification and reliable quantification of biomarkers across a large sample cohort can now be realized. In particular, as the by-products and end products of the many complex pathways present in humans and other living systems, metabolites provide a new means of holistic evaluation and indicate underlying molecular mechanisms in the context of microgravity.

In the present study, we conducted metabolic profiling and physiological detection of many parameters to demonstrate the effects of microgravity on the human body using a 45-day HDBR model. Several metabolites associated with physiological issues exhibited significant changes. Notably, although many physiological indices showed alterations in plasma, these changes were not remarkable, with $p > 0.05$. These observations reflect normal homeostasis in the human body, and their up- or down regulation by a factor of 3-5 in plasma maintains the normal distribution of biomarker concentrations (e.g., BALP, OC, and PICP) [46].

A lower weight load on the muscles and bones occurs in the absence of gravity, and a major stimulus for maintaining normal strength and endurance is lacking in microgravity environments. The HDBR model applied in the present study simulated the physiological effects of weightlessness well, and the observed changes in the levels of urinary metabolites revealed a novel molecular pathway. First, changes in BALP, OC, and PICP, which are generated during osteoblast formation, indicated that the formation of osteoblasts might be enhanced during the first 14 days to cope with weightlessness; however, osteoblast formation was reduced at R30 and R44. Comparatively, the levels of urinary *L*-threonic acid, which are strongly associated with osteoblast formation, were significantly decreased during HDBR, suggesting increased utilization of *L*-threonic acid for osteoblast formation. The recorded changes in physiological indices and metabolites indicated suppression of bone formation by HDBR, consistent with previous studies demonstrating that healthy subjects subjected to HDBR show significant suppression of bone formation [47, 48]. Second, the general loss of muscle mass during the 45-day HDBR experiment was measured at seven positions, and the total volume or maximum cross-sectional area of the muscles of different parts of the body was shown to be reduced, although these changes were not remarkable. In contrast, the excretion of urine glutamine, creatinine, glycine, and guanidoacetate, associated with muscle degradation, was significantly altered during the 45-day HDBR experiment, suggesting deconditioning of muscular tissue. Supplying free amino acids or dipeptides, such as exogenous *L*-glutamine, is an important nutritional solution for attenuating the reduced availability of glutamine in the body [28].

Furthermore, the gut microbiota present in faeces samples obtained from the experimental subjects was investigated to reveal the gut milieu of microorganisms in response to external stimuli during the 45-day HDBR experiment, based on the aerobic bacterial count. As expected, the total number of beneficial gut bacteria (*Lactobacillus* spp. and *Bifidobacterium*

spp.) initially showed a dramatic decrease, followed by an increase in the last several days. This observation might reflect the increasing urinary excretion of microbial–mammalian cometabolites (*m*-HPA and hippurate) in the first several days and decreasing urinary excretion of cometabolites in the last several days, as these two metabolites represent undesirable changes in gut microbial communities. However, a 16S rRNA or metagenomics analysis might produce more significant findings. The variations in the gut microbiome observed in the present study remain unmapped, largely reflecting limitations in analytical approaches. Several studies have suggested that changes in the microbial composition might be associated with various essential biological functions in humans.

Conclusion

Employing a different strategy than in previous studies, we investigated the effects of HDBR on humans using metabolomics, and the results showed a significant change in the urinary excretion of metabolites. In contrast to physiological indices, the variations in urinary metabolites are extensive because urine contains the elimination products of internal homeostasis. Thus, this approach is extremely useful for revealing the biochemical data of complex biofluid mixtures. In addition, the gut flora might experience significant physiological deconditioning under HDBR. While urinary microbial–mammalian cometabolites and the gut microbiota were remarkably altered, the changes in these microorganisms remain unmapped, reflecting the limitations of the applied analytical methods. Taken together, revolutionary molecular technologies for profiling the levels of molecular organization at a global level might provide an alternative to space-based research on the effects of weightlessness on humans.

Acknowledgements

This project was financially supported by grants from the State Key Lab of Space Medicine Fundamentals and Application (SMFA11A03) and the Natural Science Foundation of China (Contract No. 81202612).

Notes and references

‡ The authors declare no conflict of interests.

References

1. V. A. Convertino, *Comprehensive Physiology*, 1996, 815-843.
2. D. Roberts, X. Zhu, A. Tabesh, E. Duffy, D. Ramsey and T. Brown, *American Journal of Neuroradiology*, 2015, **36**, 2048-2054.
3. A. E. Nicogossian, C. L. Huntoon, S. L. Pool and P. Johnson, *Space physiology and medicine*, Lea and Febiger, Philadelphia, PA, 2 edn., 1988.
4. A. L. Pool-Goudzwaard, D. L. Belavý, J. A. Hides, C. A. Richardson and C. J. Snijders, *Aerospace Medicine and Human Performance*, 2015, **86**, 541-547.
5. M. Wieser, S. Gisler, A. Sarabadani, R. M. Ruest, L. Buetler, H. Vallery, V. Klamroth-Marganska, M. Hund-Georgiadis, M. Felder and J. L. Schoenberger, *Medical & biological engineering & computing*, 2014, **52**, 53-64.
6. S. Lee, A. H. Feiveson, S. Stein, M. B. Stenger and S. H. Platts, *Aerospace medicine and human performance*, 2015, **86**, A54-A67.
7. H.-z. Shi, Y.-z. Li, Z.-z. Tang, C.-f. Zhong, Q.-c. Fan, J.-y. Gao, J.-l. Liu, T. Mi, S. Zhao and Y.-h. Li, *Chinese journal of integrative medicine*, 2014, **20**, 654-660.
8. J. C. Lindon, J. K. Nicholson, E. Holmes and J. R. Everett, *Concepts in Magnetic Resonance*, 2000, **12**, 289-320.
9. M. Chadeau-Hyam, T. M. Ebbels, I. J. Brown, Q. Chan, J. Stamler, C. C. Huang, M. L. Daviglus, H. Ueshima, L. Zhao and E. Holmes, *Journal of proteome research*, 2010, **9**, 4620-4627.
10. E. A. Thévenot, A. Roux, Y. Xu, E. Ezan and C. Junot, *Journal of proteome research*, 2015, **14**, 3322-3335.
11. M. H. A. Bakar, M. R. Sarmidi, K.-K. Cheng, A. A. Khan, C. L. Suan, H. Z. Huri and H. Yaakob, *Molecular BioSystems*, 2015.
12. T. Fuhrer and N. Zamboni, *Current Opinion in Biotechnology*, 2015, **31**, 73-78.
13. V. Chubukov, L. Gerosa, K. Kochanowski and U. Sauer, *Nature Reviews Microbiology*, 2014, **12**, 327-340.
14. G. N. Gowda and D. Raftery, *Journal of Magnetic Resonance*, 2015, **260**, 144-160.
15. E. Ullah, M. Shahzad, R. Rawi, M. Dehbi, K. Suhre, M. Selim, D. Mook and H. Bensmail, *Metabolomics*, 2015, **5**, 2153-0769.100013.
16. A. L. Abuhijleh, H. A. Ali and A.-H. Emwas, *Journal of Organometallic Chemistry*, 2009, **694**, 3590-3596.
17. J. Vestergren, A. G. Vincent, M. Jansson, P. Persson, U. Ilstedt, G. Gröbner, R. Giesler and J. r. Schleucher, *Environmental science & technology*, 2012, **46**, 3950-3956.
18. R. B. Mazess, H. S. Barden, J. P. Bisek and J. Hanson, *The American journal of clinical nutrition*, 1990, **51**, 1106-1112.
19. A. A. Ferrando, C. A. Stuart, D. G. Brunder and G. R. Hillman, *Aviation, space, and environmental medicine*, 1995, **66**, 976-981.
20. K. Kailasapathy and J. Chin, *Immunology and Cell Biology*, 2000, **78**, 80-88.
21. E. Holmes, R. L. Loo, J. Stamler, M. Bictash, I. K. Yap, Q. Chan, T. Ebbels, M. De Iorio, I. J. Brown and K. A. Veselkov, *Nature*, 2008, **453**, 396-400.
22. A. Dubey, A. Rangarajan, D. Pal and H. S. Atreya, *Analytical Chemistry*, 2015, **87**, 7148-7155.
23. I. Montoliu, F.-P. Martin, P. Guy, I. Tavazzi, S. Bruce, S. Collino, V. Galindo-Cuspinera, U. Genick, N. Martin and J. Le Coutre, *Chemometrics and Intelligent Laboratory Systems*, 2010, **104**, 8-19.
24. T. M. Ebbels and R. Cavill, *Progress in nuclear magnetic resonance spectroscopy*, 2009, **55**, 361-374.
25. H.-y. Wang, P. Hu and J. Jiang, *Acta Pharmacologica Sinica*, 2011, **32**, 1555-1560.
26. A. Pavy-Le Traon, M. Heer, M. V. Narici, J. Rittweger and J. Vernikos, *European journal of applied physiology*, 2007, **101**, 143-194.
27. S. Arnaud, D. Sherrard, N. Maloney, R. Whalen and P.

Fung, *Aviation, space, and environmental medicine*, 1992, **63**, 14-20.
28. J. Tirapegui and V. F. Cruzat, in *Glutamine in Clinical Nutrition*, Humana Press, New York, 2015, pp. 499-511.
29. S. von Haehling, L. Steinbeck, W. Doehner, J. Springer and S. D. Anker, *The international journal of biochemistry & cell biology*, 2013, **45**, 2257-2265.
30. Z.-M. Wang, D. Gallagher, M. E. Nelson, D. E. Matthews and S. B. Heymsfield, *The American journal of clinical nutrition*, 1996, **63**, 863-869.
31. E. Hultman, K. Soderlund, J. Timmons, G. Cederblad and P. Greenhaff, *Journal of applied physiology*, 1996, **81**, 232-237.
32. W. J. Kraemer and J. S. Volek, *Clinics in sports medicine*, 1999, **18**, 651-666.
33. Z. Wang, E. Klipfell, B. J. Bennett, R. Koeth, B. S. Levison, B. DuGar, A. E. Feldstein, E. B. Britt, X. Fu and Y.-M. Chung, *Nature*, 2011, **472**, 57-63.
34. C. J. McEntyre, M. Lever, S. T. Chambers, P. M. George, S. Slow, J. L. Elmslie, C. M. Florkowski, H. Lunt and J. D. Krebs, *Annals of Clinical Biochemistry*, 2015, **52**, 352-360.
35. J. Marcinkiewicz and S. W. Schaffer, *Taurine 9*, Springer, 2015.
36. J. P. Muizelaar, E. P. Wei, H. A. Kontos and D. P. Becker, *Journal of neurosurgery*, 1983, **59**, 822-828.
37. J. Kołka, L. Kłinantovê, R. Kvetňanskõ, M. Marko, D. Hamar, M. Vigał and R. Hatala, *Physiological Research*, 2003, **52**, 33-339.
38. S. R. Elsden, M. G. Hilton and J. M. Waller, *Archives of Microbiology*, 1976, **107**, 283-288.
39. E. P. Nyangale, D. S. Mottram and G. R. Gibson, *Journal of proteome research*, 2012, **11**, 5573-5585.
40. J. de Vogel, W. Boersma-van Eck, A. Sesink, D. Jonker-Termont, J. Kleibeuker and R. van der Meer, *Gastroenterology*, 2006, **130**, A118-A118.
41. S. Klenow, B. L. Pool-Zobel and M. Glei, *Toxicology in Vitro*, 2009, **23**, 400-407.
42. L. J. Melton, S. Khosla, E. J. Atkinson, W. M. O'Fallon and B. L. Riggs, *Journal of Bone and Mineral Research*, 1997, **12**, 1083-1091.
43. G. Mazziotti, F. Sorvillo, M. Piscopo, M. Cioffi, P. Pilla, B. Biondi, S. Iorio, A. Giustina, G. Amato and C. Carella, *Journal of Bone and Mineral Research*, 2005, **20**, 480-486.
44. D. Nemet, T. Dolfin, I. Litmanowitz, R. Shainkin-Kestenbaum, M. Lis and A. Eliakim, *International journal of sports medicine*, 2002, **23**, 82-85.
45. C. Minkin, *Calcified tissue international*, 1982, **34**, 285-290.
46. G. L. Hortin, D. Sviridov and N. L. Anderson, *Clinical Chemistry*, 2008, **54**, 1608-1616.
47. J. M. Evans, L. C. Ribeiro, F. B. Moore, S. Wang, Q. Zhang, V. Kostas, C. R. Ferguson, J. Serrador, M. Falvo and M. B. Stenger, *European journal of applied physiology*, 2015, **115**, 2631-2640.
48. N. Goswami, J. J. Batzel and I. Valenti, in *Generation and Applications of Extra-Terrestrial Environments on Earth*, River Publishers, Delf, The Netherlands, 2015, pp. 255-265.

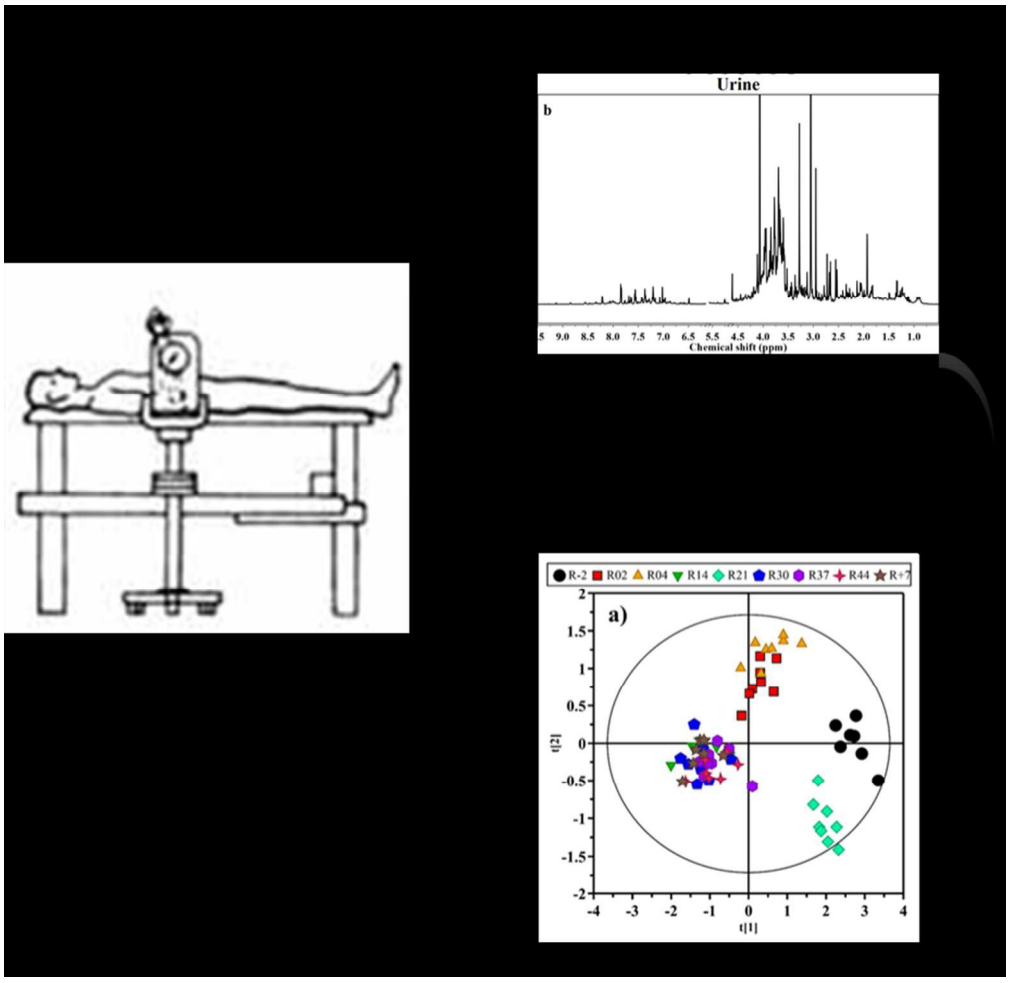

155x151mm (150 x 150 DPI)